Aberrations Measurement of Fiber-End Microlens by Free-Space Microoptical Ronchi Interferometer

C. H. Tien, C. H. Hung, and C. H. Lee

***Abstract*—We developed a microoptical Ronchi interferometer system in which a V-groove, an out-of-plane grating, a beam splitter, and a 45° upward reflector integrated on a single silicon chip were used to measure the wavefront aberration caused by a microlens on the fiber front end. By the use of the microelectromechanical systems configuration, the fringe patterns caused by the different spherical aberration and defocus balances of the 0.34-numerical-aperture microlens can be captured and analyzed accordingly. As demonstrated by the experimental results, the proposed setup is capable of carrying out a simple wavefront variation measurement in the microscopic scale.**

***Index Terms*—Integrated optics, microelectromechanical systems (MEMS), optical components, optical device fabrication.**

I. Introduction

MICROLENSES fabricated on the ends of optical fibers were first introduced by Kato for improving the coupling between light sources and optical fibers [1]. As the cost of low-loss optical fibers decreases, such schemes are widely employed in different fields of optics such as endoscopy, optical fiber sensor, and laser scanning system [2]–[4]. In order to ensure the optical performance, the fiber-end microlens or surface profile must be carefully examined. Because the fiber-end surface is so fragile and easily damaged from any scratches, it is clear that only noncontact or nondestructive approach can conduct a whole-field inspection around the optical fiber area. Among various measurements, the interferometry is the most promising technique for performing metrology or aberration testing because of its inherently subwavelength accuracy and nondestructive character. Although various interferometers have been successfully demonstrated to perform wavefront inspection [5]–[8], they are somewhat elaborate and inapplicable to the measurement of such fiber-end microlens associated with a short working distance and small radius of curvature; both are on the order of micrometers. While conducting transmitted wavefront testing, the minute working distance subject to the microlens would easily cause damage due to the contact between the front edge of the lens and the mounting accessories of the interferometric setup. On the other hand, in the refection operation, small radius convex surface of the microlens has a low reflectance; the test beam reflected from the spherical surface is no longer imaged by the objective accordingly. Recently, as the progress in the integrated circuit process, there has been growing interest in applying microelectromechanical systems (MEMS) techniques to create new optomechanical devices as well as to integrate many free-space microoptical elements on the same substrate. [9]–[11]. With sizes as small as that of a optical fiber, MEMS-based approaches have opened opportunities for state-of-art techniques to meet significant requirements of optical wavefront inspection in a microscopic scale. Three suggested approaches for the fiber-end aberration test are the Foucault knife-edge, the Ronchi grating, and the Zernike phase contrast, respectively [12]. In comparison with the conventional inteferometry, these setups need no reference beam and are easy to assemble due to their simple geometric arrangement. In all of them, the lens being tested is illuminated with a coherent beam. A modulating screen is placed in the vicinity of the focus; the aim of this screen is to alter the wavefront in some prescribed manner. Analysis of the distorted images would reveal the aberrations of the lens. For the Ronchi test, the modulating screen is a grating, which can be easily fabricated by the MEMS process and integrated with the corresponding optomechanical setup. However, to the best of our knowledge, interferometric bench incorporating MEMS grating has not been reported for such peculiar use in the study of a spherical fiber-end. To meet the specific requirement subject to on-axis image-forming by a fiber-end microlens associated with short working distance and sharp phase variation, we thus developed a simple but effective microscopic interferometer on a monolithic substrate.

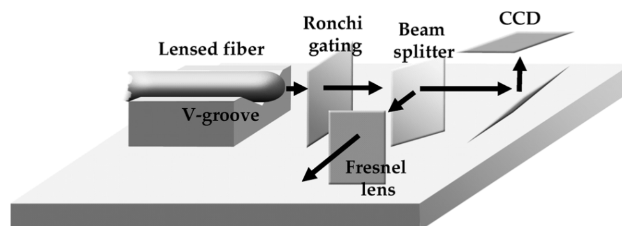

Fig. 1. Schematic drawing of the microscopic Ronchi interferometer.

II. System Design

The proposed microscopic interferometer is based on the Ronchi grating configuration. As shown in Fig. 1, light is delivered by a fiber-end microlens under test. The grating, also referred to as a Ronchi ruling, is placed perpendicular to the optical axis in the vicinity of the focus. After passing through the grating, each diffracted order will deviate from the zero order and the overlap areas of the diffracted beam will subsequently create interference fringes which characterize the aberrations of the microlens. The vertical beam splitter, with a 45° inclination

Manuscript received February 24, 2006; revised May 17, 2006. This work was supported by the National Science Council, Taiwan, for promoting academic excellence of the university in Photonics Science and Technology for Tetra Era (NSC 97-2752-E-009-009-PAE).

C. H. Tien and C. H. Hung are with Department of Photonics and Display Institute, National Chiao-Tung University, Hsinchu 30010, Taiwan, R.O.C. (e-mail: chtien@mail.nctu.edu.tw).

C. H. Lee are with Department of Photonics and Institute of Electro-Optical Engineering, National Chiao-Tung University, Hsinchu 30010, Taiwan, R.O.C.

Digital Object Identifier 10.1109/LPT.2006.880800

1041-1135/$20.00 © 2006 IEEE

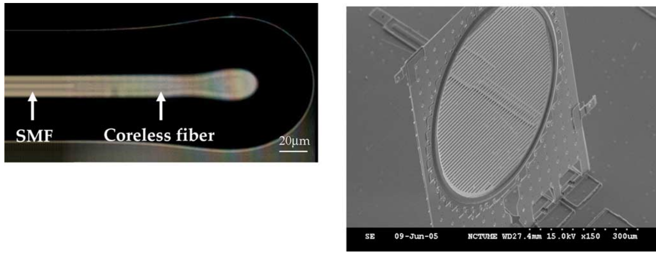

Fig. 2. (a) Side view of a hemispherical microlens on the fiber front end. (b) SEM photograph of a Ronchi grating, where the grating period has a period of $1.9 \pm 0.1\ \mu$m, corresponding to 3λ at wavelength $\lambda = 0.633\ \mu$m. (Color version available online at: http://ieeexplore.ieee.org.)

to the optical axis, splits the laser beam into two branches. One path is reflected by a 45° upward micromirror and then is captured by a charged coupled device (CCD) camera with a long-distance microscope (6×) through a frame grabber, which is placed on the top of the overall microbench. On the other hand, the other path is redirected to Fresnel lens to monitor the diffraction efficiency of each order.

The overlapping area of the fringe pattern caused by the Ronchi ruling depends on the lateral shift and it is normally expressed in terms of the numerical aperture (NA) of the microlens and the grating period P. $\mathrm{NA} = \sin\theta$, where θ is the marginal angle subtended by the exit pupil of the microlens at its focal point. In the scalar theory, the diffracted orders passing through the grating can be represented by $\sin\theta_n = n\lambda/P$, where n is the order of diffraction and θ_n is the corresponding deviation angle from the surface normal. In order to obtain a fringe pattern in high contrast, no more than two diffraction orders are allowed to overlap, so that the period of the grating P should be less than or equal to λ/NA. For the microlens on the fiber front end, we have demonstrated that the paraxial focus L and NA can be adjusted by a specific lens design [13], as shown in Fig. 2(a). Here a hemispherical microlens is fabricated on the end of a coreless fiber and serves as the focusing element. In this letter, we first designed NA of the lens as 0.33 and paraxial focus L as 100 μm when the microlens has a radius of curvature ($r = 46\ \mu$m) on an 800-μm coreless fiber. Accordingly, the period of grating was chosen to 3λ, which deviates the $\pm$1st-order diffracted beams from the zeroth-order by $\sim 19.47°$ and makes the $+$1st order just touch $-$1st order in the pupil plane distribution. The scanning electron microscope (SEM) of the out-of-plane micro-Ronchi grating is shown in Fig. 2(b), where the grating period has a period of $1.9 \pm 0.1\ \mu$m, corresponding to 3λ at wavelength $\lambda = 0.633\ \mu$m.

III. Fabrication

The overall optomechanical platform can be divided into two parts, i.e., V-groove and free-space microoptical bench. V-groove is created by KOH anisotropic etching of a (100) silicon substrate with stripe openings along the $\langle 100\rangle$ or $\langle 1\bar{1}0\rangle$ directions. Free-space microoptical bench is fabricated by surface micromachining and consists of a Ronchi grating, a beam splitter, a mirror, and a Fresnel lens. Such out-of-plane microelements were fabricated using a two-layer polysilicon and one-layer low-stress silicon nitride surface micromachining process. To fabricate the devices, a 2-μm-thick plasma-enhanced chemical vapor deposition (PECVD) silicon dioxide

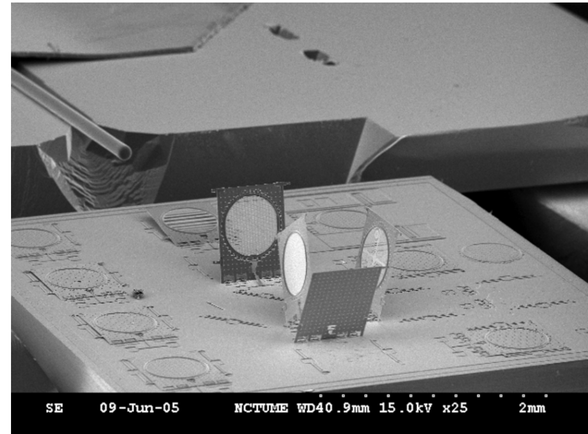

Fig. 3. SEM photograph of the microscopic Ronchi interferometer.

was first deposited on the silicon substrate as the first sacrificial layer. The 0.75-μm-deep dimples and 2-μm-deep anchors were then patterned on the sacrificial layer. The first structural polysilicon layer was deposited by low-pressure chemical vapor deposition (LPCVD) with a thickness of 2 μm. The polysilicon layer was then patterned to form a microframe. After that, a 1-μm-thick PECVD silicon dioxide, a 0.5-μm-thick LPCVD silicon nitride, and a 1-μm-thick PECVD silicon dioxide were deposited and patterned alternatively. Here the three-layer sandwich structure is used to reduce the interfacial stress of nitride and polysilicon layer. The silicon nitride optical layer was deposited with $\mathrm{SiH_2Cl_2/NH_3}$ ratio $= 3$ at 850 °C and 180 mTorr, and patterned to form various components of the optical bench. After annealing at 1150 °C for 2 h, the silicon nitride is of low stress (50 MPa) and lower absorption ($n = 2.26 + i0.033$). Then the second structural polysilicon layer was deposited with a 2-μm thickness. The polysilicon layer was then patterned to implement the microspring latches overlapping the microframe. After dicing, the structure was released in 49-wt% HF solution. The out-of-plane components were then lifted up perpendicular to the substrate and fixed by microhinges and microspring latches. Finally, the microoptical bench was assembled with a V-groove platform and optical fiber. The overall size of the microoptical bench is about 5×6 mm^2, as shown in Fig. 3.

IV. System Testing

For the Ronchi test, the fringe patterns modulated by the grating reveal the characteristics of the aberrated wavefront. In order to capture the far-field distribution, a CCD camera mounted on a microscope is used to obtain the light reflected from the upward 45° micromirror. The out-of-plane Ronchi grating ($P = 3\lambda$) is placed in the proximity of the focus of the lensed fiber. The optical fiber is attached on a piezoelectric transducer (PZT) separated from the optical bench. Therefore, the relative distance between the microlens and the grating can be adjusted by the PZT and subsequently create a wavefront associated with different aberration balances. Since each optical element and corresponding setup is precisely aligned by the foundry process, the accuracy of the system is comparable with the conventional instrument. It is beyond the scope of this letter to discussion various aberrations caused by the fabrication error during the discharge arc process; in this study, we were

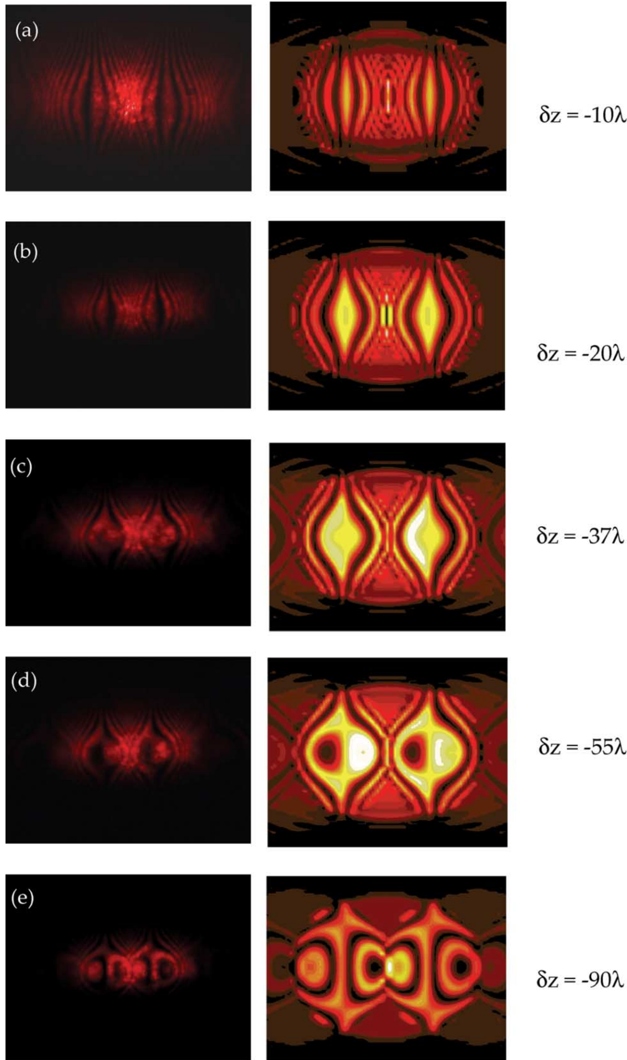

Fig. 4. Measured (left column) and calculated (right column) patterns of intensity distribution when the Ronchi grating was placed in different place $\delta z = -10\lambda$, -20λ, -37λ, -55λ and -90λ, respectively. Where δz is the axial shift of the grating position with respect to the paraxial focus, negative distances are towards the marginal focus. (Color version available online at: http://ieeexplore.ieee.org.)

treating only the case where the center of the incident Gaussian field coincides with the optical axis, only defocus and on-axis aberration such as spherical aberration (SA) are presented. For optical testing, the wavefront deformation W (or optical path difference) in the normalized exit pupil (x, y) of the microlens with respect to the paraxial focal point can be presented as $W(x,y) = C_{040}(x^2 + y^2)^2 + C_{020}(x^2 + y^2)$, where C_{040} and $C_{020} = 0.5(\mathrm{NA})^2\delta z$ are the primary third-order SA and defocusing terms, respectively. Where δz is the axial shift of the grating position with respect to the paraxial focus, negative distances are towards the marginal focus. Left column in Fig. 4 shows the measured fringes subject to different balances between the SA and defocus, where the Ronchi grating was placed at $\delta z = -10\lambda$, -20λ, -37λ, -55λ, and -90λ, respectively. In the process, as the grating shifts through the paraxial focus and towards the marginal focus, we observed a rich variety of third-degree curves that aid us in determining the wavefront is indeed predominated by the third-order SA.

It is noted that there is a small overlapping portion of the ± 1st beams, meaning that the NA of the lens under test is no longer equal to λ/P but a little higher than the designed value 0.33. The reason is due to that the fabrication of the lensed fiber via high-frequency discharge arc is hard to precisely control its vertex curvature, resulting in a smaller radius ($r = 45\ \mu$m) than the designed value ($r = 46\ \mu$m). Frame (a)–(e) in right column of Fig. 4 corresponds to the calculated results at different values of δz under NA $= 0.34$, $C_{040} = 4.86\lambda$. The close agreement with the experimental cubic fringes confirms the characteristics of such microoptical system and quantitatively ensures the merits of the fiber-end microlens. If the wavefront analysis can be further implemented by a polynomial least-square fitting algorithm, such MEMS-based interferometric bench is expected to be comparable with the conventional interferometer in terms of resolution and accuracy.

V. Conclusion

We have developed a free-space Ronchi interferometer by the surface micromachining and experimentally verify its feasibility for optical wavefront aberrations measurement of a fiber-end microlens system. We fabricated a microlens associated with NA $= 0.34$ and SA $(\mathrm{SA}) = 4.86\lambda$ as a testing sample and successfully observed the fringe patterns due to the various SA and defocus balances. The similar analyses can be performed for any reasonable number of aberrations as well. Compared with the conventional interferometer whose sizes are several hundred times larger than that of an optical fiber, the MEMS-based interferometric bench offers the potential to perform fast, in-line, noncontact, and precision measurement of the microlens inspection in the microscopic scale.

References

[1] D. Kato, "Light coupling from a strip-geometry GaAs diode laser into an optical fiber with spherical end," *J. Appl. Phys.*, vol. 44, pp. 2756–2758, 1973.
[2] K. S. Lee and F. S. Barnes, "Microlens on the end of single-mode optical fibers for laser applications," *Appl. Opt.*, vol. 24, no. 19, pp. 3134–3139, 1985.
[3] L. Giniunas, R. Juskaitis, and S. V. Shatalin, "Endoscope with optical sectioning capability," *Appl. Opt.*, vol. 32, no. 16, pp. 2888–2890, 1993.
[4] E. Udd, "Fiber optic smart structures," *Proc. IEEE*, vol. 84, no. 6, pp. 884–894, Nov. 1996.
[5] G. W. R. Leibbrandt, G. Harbers, and P. J. Kunst, "Wave-front analysis with high accuracy by use of a double-grating later shearing interferometer," *Appl. Opt.*, vol. 35, no. 31, pp. 6151–6161, 1996.
[6] J. C. Wyant, "Double frequency grating lateral shearing interferometer," *Appl. Opt.*, vol. 12, no. 9, pp. 2057–2060, 1973.
[7] P. Hariharan, "Optical interferometry," *Rep. Prog. Phys.*, vol. 54, pp. 339–390, 1990.
[8] T. Yatagai, "Fringe scanning Ronchi test for aspherical surface," *Appl. Opt.*, vol. 23, no. 20, pp. 3676–3679, 1984.
[9] M. C. Wu, "Micromachining for optical and optoelectronics systems," *Proc. IEEE*, vol. 85, no. 11, pp. 1833–1856, Nov. 1997.
[10] M. C. Wu, L. Y. Lin, S. S. Lee, and K. S. J. Pister, "Micromachined free-space integrated micro-optics," *Sens. Actuators: A (Phys.)*, vol. 50, pp. 127–134, 1995.
[11] S. S. Lee, L. S. Huang, C. J. Kim, and M. C. Wu, "Free-space fiber-optic switches based on MEMS vertical torsion mirrors," *J. Lightw. Technol.*, vol. 17, no. 1, pp. 7–13, Jan. 1999.
[12] A. Cornejo-Rodriguez, "Ronchi test," in *Optical Shop Testing*, D. Malacara, Ed., 2nd ed. New York: Wiley, 1992, pp. 321–365.
[13] C. H. Tien, Y. C. Lai, T. D. Milster, and H. P. D. Shieh, "Design and fabrication of fiberlenses for optical recording applications," *Jpn. J. Appl. Phys.*, vol. 41, pp. 1834–1837, 2002.